

Transfer Cavity Stabilization Using the Pound-Drever-Hall Technique with Noise Cancellation

by

Mozhgan Torabifard

A thesis
presented to the University of Waterloo
in fulfillment of the
thesis requirement for the degree of
Master of Science
in
Physics

Waterloo, Ontario, Canada, 2010

© Mozhgan Torabifard 2010

I hereby declare that I am the sole author of this thesis. This is a true copy of the thesis, including any required final revisions, as accepted by my examiners.

I understand that my thesis will be made electronically available to the public.

Abstract

A system for exciting Rubidium atoms to Rydberg states has been constructed to study the interactions between them and metal surfaces. This thesis describes a method to reach the f Rydberg series using diode lasers. Since the diode lasers need to be frequency stabilized for this excitation, a transfer cavity stabilization method was implemented using the Pound-Drever-Hall technique.

To obtain the necessary frequency modulation the diode laser was current modulated at ~ 6 MHz. A noise cancellation circuit was used to suppress detection of the accompanying residual intensity modulation.

Acknowledgements

I would like to express my genuine appreciations to my supervisor, Dr James Martin for his guidance, and support throughout my research. I learned a great deal from his knowledge and hardworking.

I would like to extend my grateful acknowledgment to my thesis examination committee, David Yevick and Donna Strickland for their time and comments on this work.

My special thanks to the administrative staff of the Physics Department of the university of Waterloo. I would like to thank Zhenwen Wang and Harmen Vander Heide and Hiruy Haile for their help. I also grateful to Martin's group members, Jeffrey David Carter and Lucas Jones for their help and support during my project.

Many Thanks to my family for the immortal love and care, which always shined on me far from home. Finally and most importantly, I thank my dear fiance, Omid Aminfar for his care, love and understanding.

Dedication

To Omid

for all your support and and inspiration

Table of Contents

List of Figures	x
1 Introduction	1
1.1 Rydberg atoms	1
1.2 Excitation of Rb atoms	2
1.2.1 Excitation Problems	3
1.2.2 The proposed method for excitation	4
1.3 Diode laser	5
1.3.1 External Cavity Diode Lasers	5
1.3.2 Negative Feedback Control	7
1.4 Locking The Diode Lasers	8
1.5 Noise Cancelation	9
2 Noise Cancellation	10
2.1 Introduction	10
2.2 Noise suppression	10

2.3	Noise Cancellation Circuit	12
2.4	The performance	13
2.4.1	Photodiode Saturation	14
2.4.2	The Noise Cancellation Circuit Performance	16
3	Locking System	21
3.1	Introduction	21
3.2	Optical Cavity Stabilization	22
3.3	The Pound-Drever-Hall Laser Frequency Stabilization System	24
3.4	Using the PDH System to Stabilize an Optical Cavity by a Doubly Current Modulation Injection Locked Diode Laser	27
3.5	Modulation Signal Generation	30
3.5.1	Generating Waveform	30
3.5.2	Transferring	31
3.6	Current Modulation of the diode laser	33
4	Experiment	34
4.1	Experimental Setup	34
4.2	Measurements	39
5	Summary and Suggestions for Future Works	44
	Bibliography	48

List of Figures

1.1	Optical excitation scheme for Rubidium atoms in two steps	2
1.2	Proposed optical scheme to excite Rubidium atoms to Rydberg states . . .	4
1.3	The hyperfine levels for ^{85}Rb and ^{87}Rb frequency spacing in MHz	6
1.4	A pseudo-external cavity laser using a standard commercial laser and a diffraction grating for feedback	7
1.5	Allowable transitions between the $5p_{3/2}$ and $5d_{5/2}$ states of ^{87}Rb	8
2.1	Diagram of a generic laser noise suppression scheme. The noise improvement comes from the combining signal and comparison photocurrents	11
2.2	Schematic diagram of the basic noise cancellation	12
2.3	Photodiode capacitance as a function of bias voltage and size active area. . . .	14
2.4	RF power at 6 MHz as a function of light power. The straight line corresponds to linear behavior. Here linear behavior means RF power is proportional to the square of DC light power.	15
2.5	Schematic diagram of the new noise cancellation circuit	16
2.6	Measured 1 MHz cancellation performance of the circuit of Fig. 2.5 with THAT340 transistors as a function of the log ratio output voltage.	18

2.7	Measured 6 MHz cancellation performance of the circuit of Fig. 2.5 with THAT340 transistors as a function of the log ratio output voltage.	19
2.8	Cancellation performance at 6 MHz of the circuit of Fig. 2.5 without cascode transistor Q_3 . THAT340 is used for Q_1 and Q_2 (two NPNs).	19
2.9	The suppression of the signal by the circuit of Fig. 2.5 which used $0.2 \mu\text{F}$ instead of $2\mu\text{F}$ in the feedback part.	20
2.10	The performance of the circuit of Fig. 2.5 with HFA3096BZ-ND transistors.	20
3.1	Adding a tunable sideband to one laser making the fringes coincide.	23
3.2	Experimental setup employed by Bohlouli-Zanjani et al	24
3.3	Intensity and phase of the reflection beam for Fabry-Perot cavity	26
3.4	The Pound-Drever-Hall error signal for high modulation frequency and ideal phase condition	27
3.5	Schematic of how the Pound-Drever-Hall method is applied to stabilize the transfer cavity using the secondary sidebands (green) as a PDH sidebands for a primary tunable sideband (red) of the slave laser	29
3.6	Part a: The system for generation of the slave laser current modulation. AWG: Arbitrary waveform generator, VCA: Voltage controlled attenuator. Part b: The system for preparing the reference signal for demodulation.	32
4.1	Experimental setup. PBS: polarizing beam splitter, PD: photodiode,FR: Faraday rotator, NPBS: None-polarizing beam splitter.	36
4.2	The error signal of reflected beam for the 780 nm laser with different frequencies of modulation using the noise cancellation circuit.	39

4.3	Absorption spectrum for the $5p_{3/2}$ to $5d_{5/2}$ of ^{87}Rb transition and the associated error signal obtained by scanning the carrier modulation frequency of the slave laser. In this measurement the noise cancellation circuit is used only for the 780 nm laser	40
4.4	Drift frequency of the 775 nm laser over time. In this measurement the noise cancellation circuit was used only for the 780 nm laser	41
4.5	Absorption spectrum for the $5p_{3/2}$ to $5d_{5/2}$ transition of ^{87}Rb and the associated error signal obtained by scanning the carrier modulation frequency of the slave laser. In this measurement the noise cancellation circuits are used for measuring both the 780 nm and 775 nm lasers	42
4.6	Drift frequency of the 775 nm laser over time. In this measurement noise cancellation circuits are used for both the 780 nm and 775 nm lasers	43

Chapter 1

Introduction

1.1 Rydberg atoms

A Rydberg atom is an atom with a valence electron which has been excited to a high principal quantum number n . The Rydberg atom consists of a loosely bound electron which orbits around a positive ionic core. Therefore its atomic structure and properties are very similar to Hydrogen. Because of the hydrogenic nature of Rydberg atoms, the energies of these excited atoms are well defined by the Rydberg formula, with n replaced by an effective principal quantum number n^* which depends on the quantum defect δ_l of the state of the angular momentum l [1].

Rydberg atoms have properties that scale systematically with n ; for example the excited state lifetime scales as n^3 . Since the electric polarizability scales as n^7 , the spectroscopy of these atoms can be used to detect very small electric fields [2]. These remarkable properties of Rydberg atoms make them a good choice for studying interactions between atoms and surfaces. For these purposes Rubidium atoms (the valence electron is at $n = 5$) are excited to Rydberg states close to $n = 50$.

1.2 Excitation of Rb atoms

One of the ways to excite Rubidium atoms to Rydberg states is a two-step excitation method [1]. This excitation scheme, which is employed to cool and trap these atoms and excite them to Rydberg states is shown in Fig. 1.1.

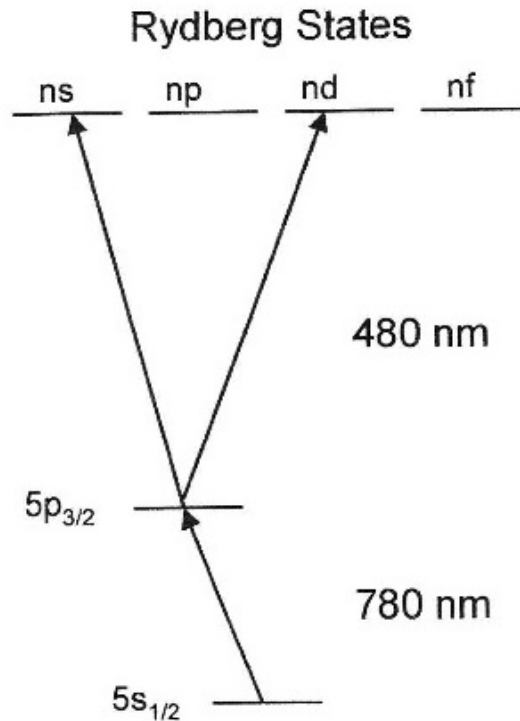


Figure 1.1: Optical excitation scheme for Rubidium atoms in two steps

In the first step, the Rubidium atoms are excited from the ground state $5s_{1/2}$ to the first excited state $5p_{3/2}$ using a 780 nm diode laser. The next excitation to different Rydberg states, was done by a frequency doubled Ti:Sapphire laser (approximately 480 nm) [3].

1.2.1 Excitation Problems

A few problems are anticipated with using this technique to study Rydberg atom metal surface interactions.

- ***Photoelectrons***

Since the energy of photons with a wavelength of 480 nm is higher than the work function of many metals, using this light near metal surfaces can cause electrons to be emitted from the surface. Consequently these electrons will collide with the Rydberg atoms which may ionize them, resulting in inaccurate Rydberg spectroscopy measurements.

- ***No access to the f levels Rydberg states from the $5p_{3/2}$ level***

As Fig. 1.1 shows, only an excitation from $5p_{3/2}$ to the s and d series of Rydberg states are possible. Since in the presence of an applied electric field a state of higher angular momentum exhibits stronger quadratic Stark shifts, accessing the f series can enhance the sensitivity to the electric field. Subsequently the two-step excitation method restricts the sensitivity of measurements [4].

- ***Short lifetime of the $5p_{3/2}$ state***

A radiative broadening mechanism is added to the linewidth of spectroscopy measurements due to the finite lifetime of the energy levels. The short lifetime of the $5p_{3/2}$ state results in a natural line width on the order of 6 MHz.

- ***High Cost***

Light with a 480 nm wavelength is not directly accessible by laser diodes. Expensive laser systems such as a Ti:Sapphire ring laser are required to provide this wavelength.

1.2.2 The proposed method for excitation

Using the $5d_{5/2}$ state in the excitation process can solve the aforementioned problems. In this method after exciting atoms from the $5s_{1/2}$ to the $5p_{3/2}$ state, they are driven to $5d_{5/2}$ using a 776 nm light. Finally the Rydberg atoms are excited with ~ 1260 nm light. This scheme is demonstrated in Fig. 1.2.

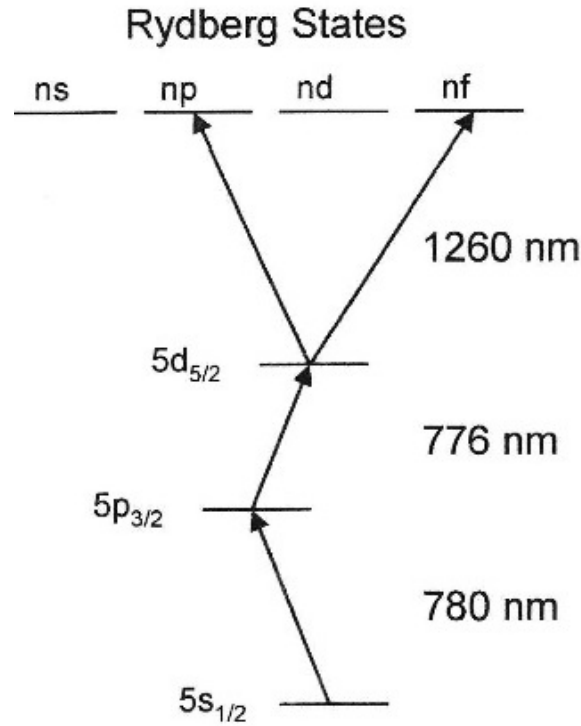


Figure 1.2: Proposed optical scheme to excite Rubidium atoms to Rydberg states from Ref. [5].

- As the energy of the photon with a 776 nm or 1260 nm wavelength is below the work function of metals, the photoelectric effect should not be a problem.
- Since the atoms are excited to the Rydberg states from the $5d_{5/2}$ state, transitions to the f series are allowed. This enhances the sensitivity to electric fields.

- Due to longer lifetime of the $5d_{5/2}$ state as compared to the $5p_{3/2}$ state (10 times), the natural line width of a spectroscopic measurement can be reduced by approximately 10 times [6].
- Inexpensive diode lasers are available for 776 nm and 1260 nm wavelengths [5].

1.3 Diode laser

Tunable diode lasers are the most common type of lasers in atomic physics, since they are sources of narrow-band light and are less expensive than dye or Ti-sapphire lasers. This type of laser typically has an output with tens of MHz width. It is possible to tune them continuously over desired regions. Reference [7] is an excellent reference for using diode lasers in atomic physics which explains the use of the optical feedback technique to control these lasers and describes applications of these techniques in various areas of atomic physics. References [8] and [9] discuss the stabilization of lasers by implementing the external cavity and grating feedback methods.

As Fig. 1.3 shows, the difference in energy levels for the hyperfine states of $5d_{5/2}$ range from a few MHz to tens of MHz. In this condition a stabilized diode laser with a line-width on the order of MHz is needed.

Since free-running single mode diode lasers typically have line-widths of the order of 10 MHz and their mode-hop free tuning is poor at best, improvements are needed for diode lasers to use them in Rydberg atom experiments.

1.3.1 External Cavity Diode Lasers

Several methods including optical and electrical ones can improve laser line-width and control wavelength. An external cavity configuration can select and tune the emission

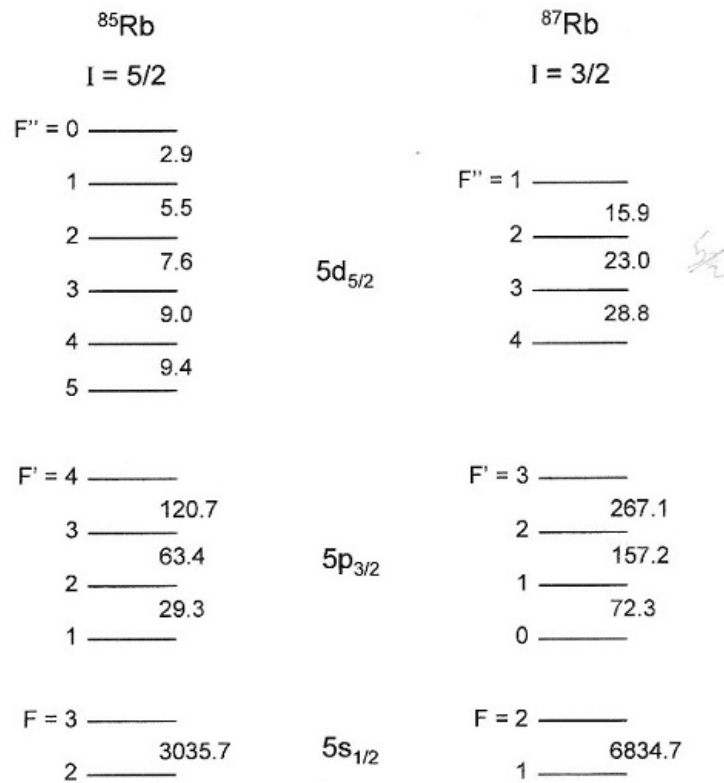


Figure 1.3: The hyperfine levels for ^{85}Rb and ^{87}Rb frequency spacing in MHz (from Ref. [10]).

wavelength by using antireflection coating on the diode laser chip and some external optical devices [7]. Figure 1.4 shows the configuration of an external cavity.

Using a diffraction grating, an optical resonator cavity is formed. Consequently only those frequencies that are resonant modes of the cavity are emitted. These frequencies can be varied by adjusting the cavity length, which can be done using a piezoelectric transducer (PZT). Narrow line-widths on order of the MHz and excellent tunability can be achieved with external cavity diode lasers [8].

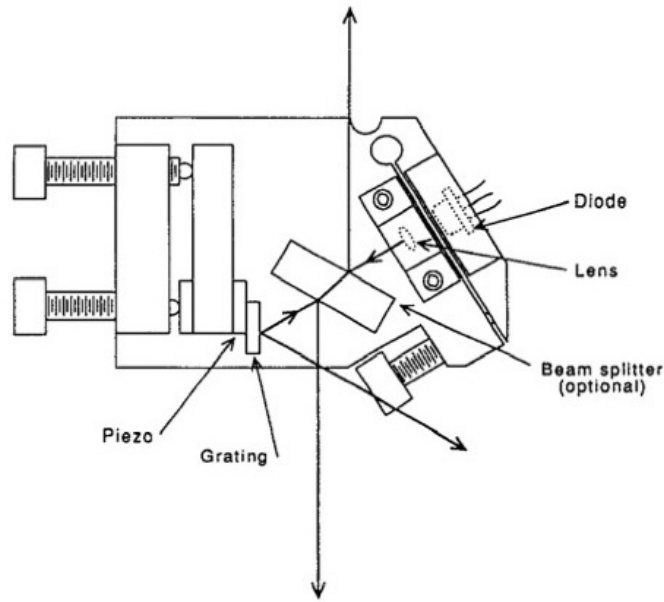


Figure 1.4: A pseudo-external cavity laser using a standard commercial laser and a diffraction grating for feedback (from Ref. [8]).

1.3.2 Negative Feedback Control

Continuously adjusting of the optical cavity length by implementing the negative feedback control method can avoid any change in the laser's frequency . This method minimizes the laser's sensitivity to temperature, current and vibration. This technique also gives the ability to stabilize the external cavity diode laser to a specific frequency. By measuring a portion of the output beam, a signal which identifies the deviation from the specific frequency is provided. This specific frequency can be an atomic transition or a resonant cavity mode. In order to use the signal to adjust the PZT, it is required to convert that into an error signal by a lock-in detection system [7].

1.4 Locking The Diode Lasers

As mentioned in Section 1.2 this excitation method has three steps. In the first step an external cavity diode laser can be used which is locked by Rb saturated absorption spectroscopy using a vapor cell. In the second step, eight transitions are allowed according to the selection rules for hyperfine transitions between the $5p_{3/2}$ and $5d_{5/2}$ states, as shown in Fig. 1.5.

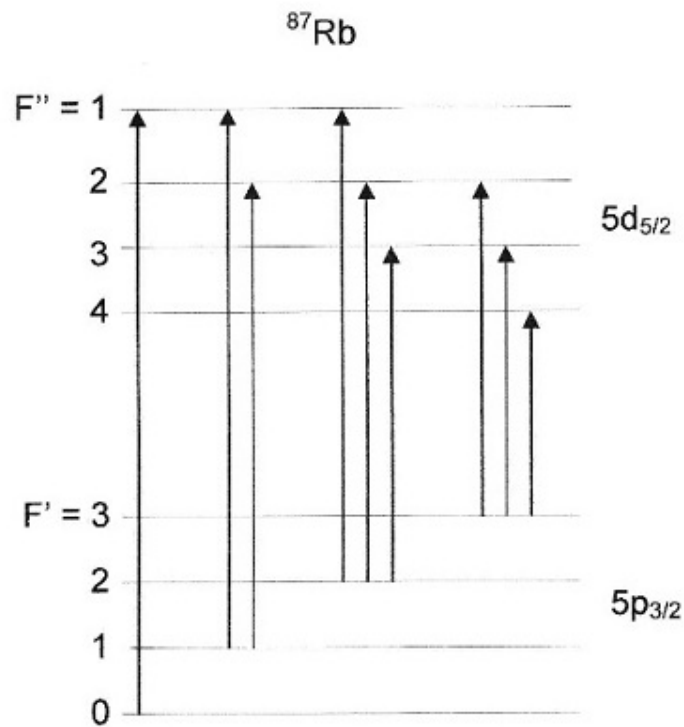


Figure 1.5: Allowable transitions between the $5p_{3/2}$ and $5d_{5/2}$ states of ^{87}Rb .

These transitions can be observed using two-photon spectroscopy in a vapor cell. Examples of this method are given in [11] and [12]. The two-photon spectroscopy allows the 775 nm diode laser's frequency to be stabilized to the transition of the Rb atoms between the $5p_{3/2}$ to $5d_{5/2}$ states. In the last step of the Rydberg state excitation, a frequency stabilized diode laser at 1260 nm is needed. Since there is no direct transition to be used as a reference

for this wavelength, an optical transfer cavity can be employed to lock the diode laser. In Chapter 3 the method of locking the 1260 nm diode laser will be introduced. In this method, the Pound-Drever-Hall locking system [13] improves the laser's frequency stability. A transfer cavity is stabilized by locking to the modulation sideband of a reference laser (a 780 nm diode laser) and then the target laser (a 1260 nm diode laser) is locked to the stabilized cavity. Injection current modulation is applied to both lasers. A new scheme is used to generate the modulation signal which is injected to the target laser. Applicability of this method is tested by using a 775 nm external cavity diode laser instead of the 1260 nm diode laser, as described in Chapter [4].

1.5 Noise Cancelation

The residual intensity modulation which is caused by the frequency modulation (FM) required for the Pound-Drever-Hall technique creates an undesired baseline in the error signal. The subtractor method employes a small part of the beam which does not interact with the cavity as a comparison beam and suppresses this baseline in measurements. The comparison beam should have the same power as the signal beam. In previous work, a polarization beam splitter was used to manually balance the beams (comparison and signal) that were going into two photodiodes from which the current difference is amplified. This method causes slow baseline drifts, particularly when the spatial properties of the beam for the cavity locking system is cleaned up by a fiber. An improvement to this method using a negative feedback signal which provides the continuous adjustment of the DC balance between the two aforementioned beams will be described in Chapter 2.

Chapter 2

Noise Cancellation

2.1 Introduction

Spurious optical signals and power drifts are problems in majority of optical measurements. There are a great variety of ways in which laser noises arises. Mode hopping and power fluctuations caused by the current modulation are some examples of noise which prevents precise measurements. Since some experiments require accurate optical measurements, efforts have been made to minimize the noise in optical systems. A method to eliminate excess laser noise developed by Hobbs [14, 15].

2.2 Noise suppression

Noise suppression methods are based on comparing a signal beam to a comparison beam (reference beam). In this kind of measurement, both the signal photocurrent and a static background are measured while both of them are proportional to the laser power. Figure 2.1 shows the schematic for this method. Although there is no attempt to stabilize the laser beam in this method, the sample beam is detected for comparison between these

two beams both have the same fractional noise. These two beams to be combined to obtain an output current that completely is free of excess noise. Subtraction and division have been common methods to address this issue.

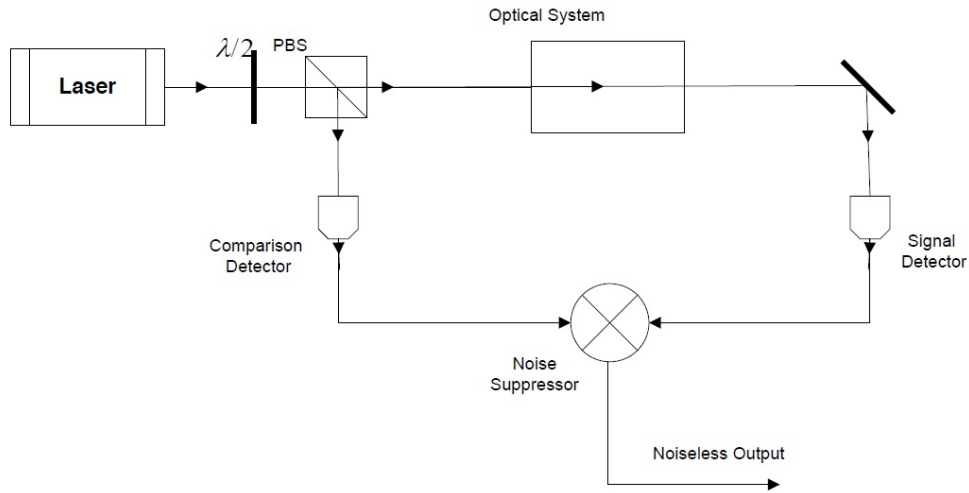


Figure 2.1: Diagram of a generic laser noise suppression scheme. The noise improvement comes from the combining signal and comparison photocurrents

In the subtractive method, the comparison photocurrent is subtracted from the signal current [16]. Both of these photocurrents are equal in power if the optical system is adjusted perfectly which leads to cancellation of the excess noise and DC current. Subtractors can have wide band-widths since the subtraction can be done directly. A suppression of more than 20 dB can be reached by this method, but because the intensity of the signal beam often changes during the measurements, these two currents can not be equal always. Therefore it is required to adjust the power of the reference beam. In this method it is possible to replace the optical adjustment device with an electronic one as explained in the next section.

On the other hand, this adjustment is not required for dividers. Since the two beams are both proportional to the laser power, the output signal is normalized out of the noise

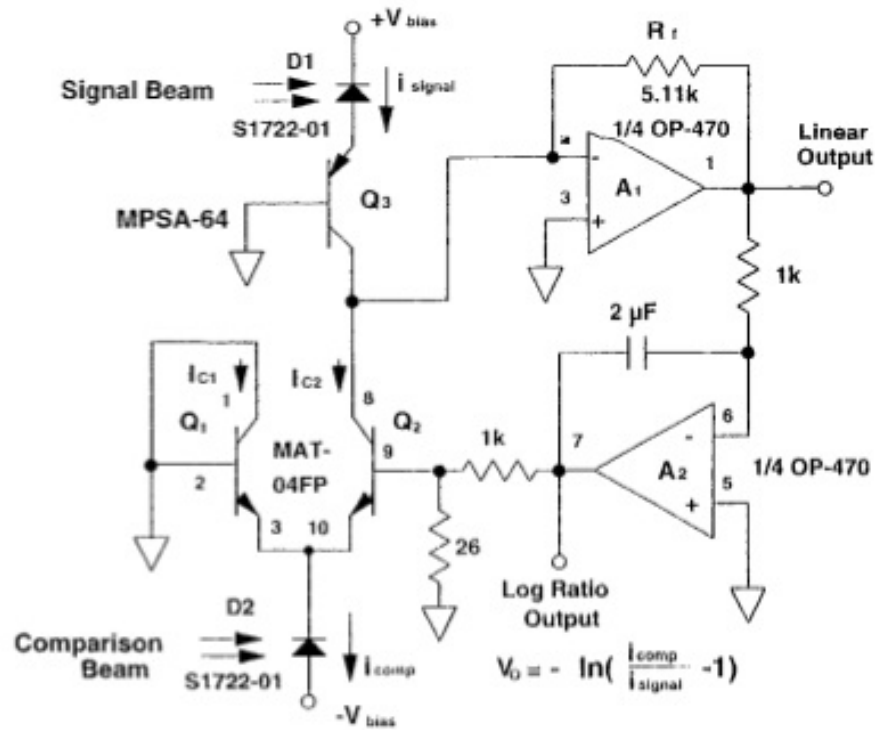


Figure 2.2: Schematic diagram of the basic noise cancellation (from Ref. [15]).

by dividing the signal beam by the sample one. Because dividers tend to be slow, the suppression bandwidth is limited in this method [17].

2.3 Noise Cancellation Circuit

The subtractor method can be improved significantly by using negative feedback to have continuous adjustment of the DC balance between the signal beam and the comparison beam [18].

As stated in Ref. [15], "Feedback control requires an electronically variable current splitter between the signal and comparison photocurrents and electronic criterion for when

the circuit is in balance”. Figure 2.2 is a schematic of a device which applies this idea. By arranging the optical system to have the comparison beam stronger than the signal beam and dividing the comparison beam into two parts by employing a bipolar transistor pair (Q_1 and Q_2) the DC balance can be achieved. The splitting ratio is adjusted by negative feedback. Besides the $Q_1 - Q_2$ pair, there is a transimpedance amplifier A_1 which converts the current to the voltage. The integrating servo amplifier A_2 forces the DC output of A_1 to be zero by controlling the ratio of the comparison beam deviation. The cascode transistor Q_3 prevents the capacitance of the signal photodiode from loading the summing junction. In this circuit, since the DC photocurrent is canceled, the large feedback resistors can be used without saturating amplifier A_1 . Any fluctuations in the comparison beam are exactly divided by the same ratio as DC, which is caused by the transistor behavior, while it does not relate to the feedback loop bandwidth. Thus the cancellation bandwidth is independent of the feedback loop bandwidth.

Since the noise fluctuations of the photocurrent are exactly proportional to its DC value, the negative feedback to the transistor Q_2 keeps the DC value of the linear output at zero. There is an alternative output called the log ratio output which is related to the ratio of the comparison current to the signal current, with:

$$V_0 = -\ln\left(\frac{I_{comp}}{I_{signal}} - 1\right). \quad (2.1)$$

If this output is used as the main output, the circuit works as a divider.

2.4 The performance

Previous workers in the lab used subtraction of the signal and reference beam photocurrents to suppress the baseline due to residual intensity modulation. The reference beam must have exactly the same power as the signal beam. A polarization beam splitter and a half wave plate were used to manually balance the beams (reference and signal) and the

current difference was amplified. The noise cancellation circuit of Hobbs does not require manual adjustment. Thus we implemented this circuit.

2.4.1 Photodiode Saturation

The following experiment is designed to investigate which photodiode should be used in the noise cancellation circuit. In general high photodiode capacitance reduces bandwidth. Although it is possible to partially compensate for this with more complicated circuits, it is best to minimize capacitance. Photodiode capacitance increases with active area. However

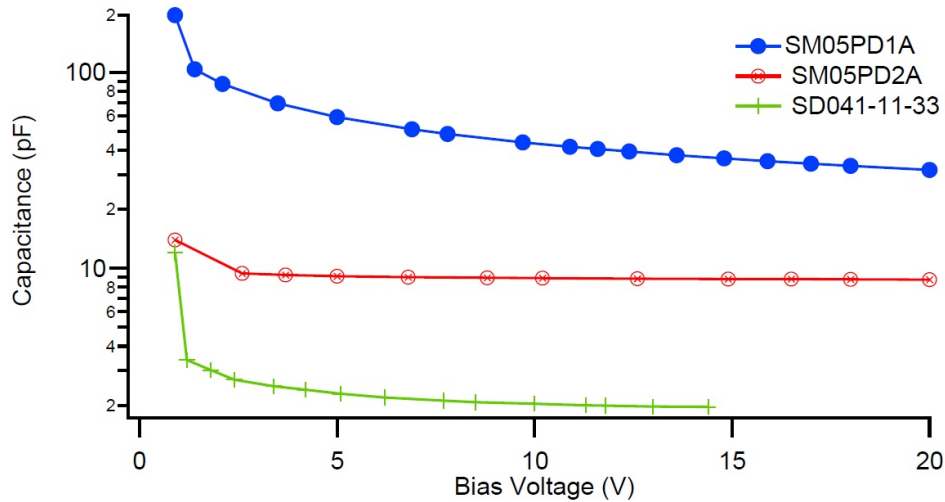


Figure 2.3: Photodiode capacitance as a function of bias voltage and size active area.

smaller photodiodes saturate at lower optical power. For example Philip Hobbs in his book, "Building Electro-Optical Systems" (see in Ref. [19]), mentions that 1 mA photo current in a 3 mm photodiode leads to saturation. Because very little quantitative information on photodiode saturation was found, the capacitance and the saturation properties of three photodiodes were measured. Two of the photodiodes are from ThorLabs: a large one (P/N SM05PD1A) with 13 sq mm active area and small one (P/N SM05PD2A) with 0.8 sq mm active area. The third photodiode is P/N SD041-11-33 from Advanced Photonix

Inc and 0.83×1.02 mm active area. Current modulation is applied at 6 MHz to a 780nm external cavity diode laser (Toptica, DL100 with FET- current modulation). The resulting frequency modulation leads to an oscillating photocurrent at 6 MHz in the photodiodes. Two different beam sizes are used at the photodiodes. Using knife edge measurements and assuming a gaussian profile, w , the $1/e$ amplitude radii are 6.78 mm and 1.13 mm. The smaller size is used for the two smaller photodiodes and both sizes are used for the larger photodiode. The power of the beam is varied using a variable attenuator and measured with a power meter. The photodiode is biased with +15 V using a bias-T and the RF signal at 6 MHz is amplified using two ZFL-500(MiniCircuits) amplifiers. The signal amplitude is measured using a spectrum analyzer. As Fig. 2.4 shows, the SD041-11-33 photodiode

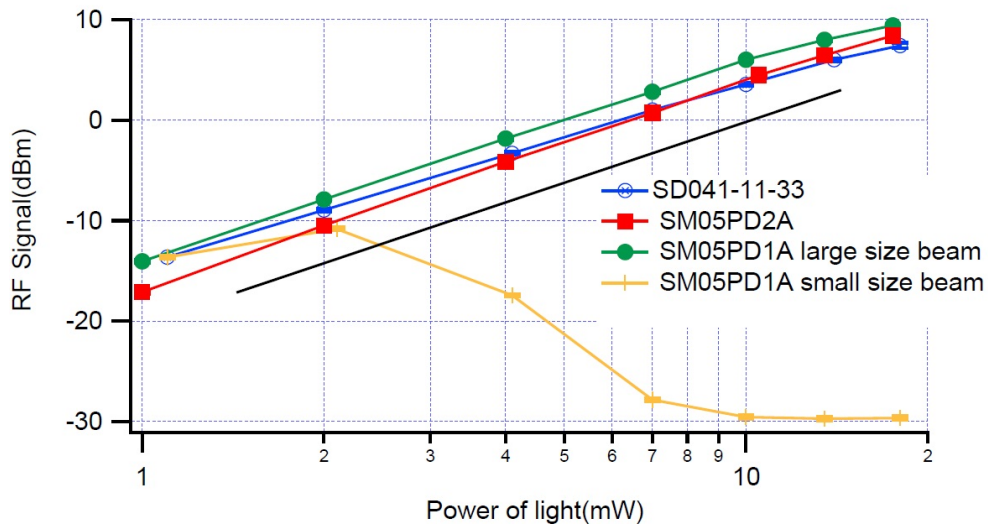


Figure 2.4: RF power at 6 MHz as a function of light power. The straight line corresponds to linear behavior. Here linear behavior means RF power is proportional to the square of DC light power.

shows more saturation than the two other photodiodes. In addition, decreasing the size of the beam incident on the photodiode leads to more saturation.

In conclusion, SM05PD2A is the best photodiode for the noise cancellation circuit

because of two reasons:

1. It has lower capacitance than the SM05PD1A photodiode.
2. It is less saturated than the SD041-11-33 photodiode at 2 mW.

2.4.2 The Noise Cancellation Circuit Performance

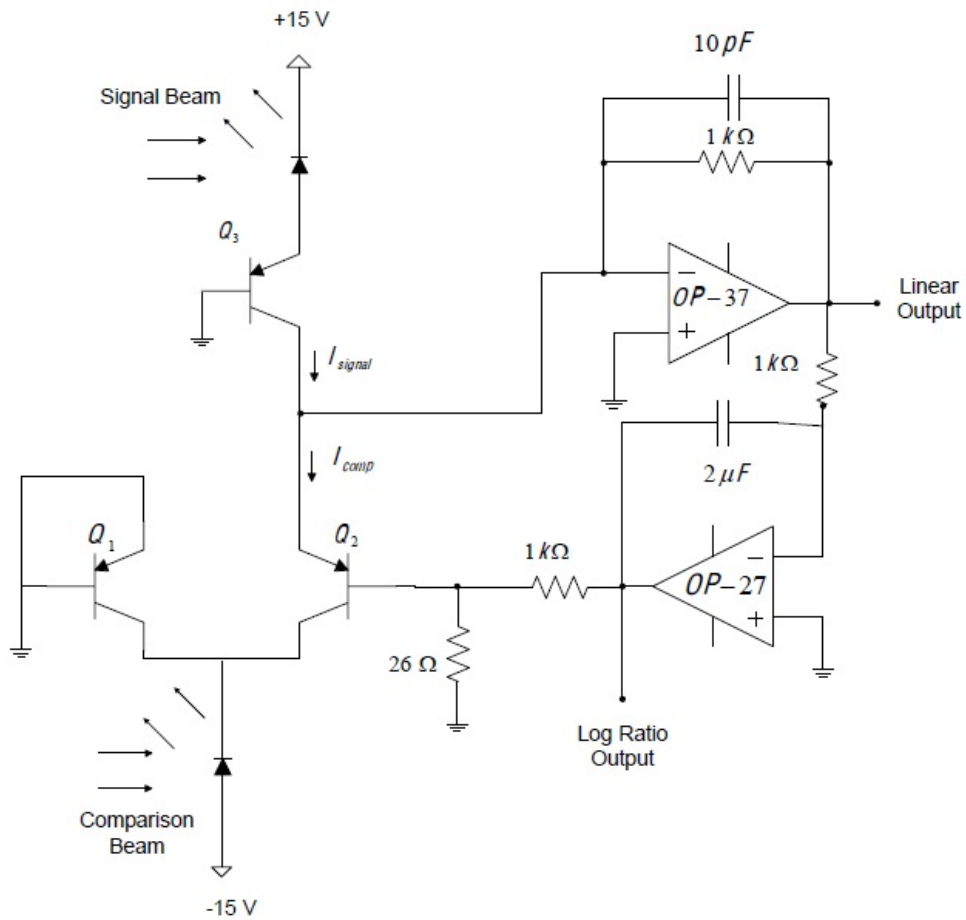


Figure 2.5: Schematic diagram of the new noise cancellation circuit

Figure 2.5 shows the components which are implemented in the new noise cancellation circuit. The FDS010 photodiode (Thorlabs, P/N FDS010) which is the unmounted ver-

sion of SM05PD2A is employed in this circuit based on the conclusion from Subsection [2.4.1]. As shown in Fig. 2.3, the capacitance of this photodiode is $\sim 10pF$ at 15 V bias voltage. The photodiode's capacitor tends to destabilize the circuit. To avoid reduction in the bandwidth of A_1 , a 10 pF capacitor should be applied in parallel with R_f in the feedback loop. Figures 2.6 and 2.7 show the performance of this circuit for a variety of signal beam powers (current signal) at 1 and 6 MHz in which the circuit's transistors are THAT 340 (NPNs are used for matched pair, and the PNP used for cascode). In all the measurements, an external cavity diode laser at 775 nm is directly frequency modulated by a wave generator (Aligent, P/N 33200A). The resulting frequency modulation leads to an oscillating photocurrent at the modulation frequency in the photodiodes. A polarization beam splitter splits the beams. The power of the beams are varied using a variable attenuator and measured with a power-meter.

The data is from a spectrum analyzer; one sweep is taken with canceler operating normally and a second sweep with the comparison beam blocked. These plots show the difference between these two sweeps. Different log ratio outputs are achieved by changing the comparison beam (Equation 2.1). This process is repeated for different powers of the signal beam.

Since the response of the photodiode at 775 nm is $\sim 0.5\frac{A}{W}$, the optical power is measured and the current signal is obtained.

As shown in Fig. 2.6 and Fig. 2.7, it is difficult to predict a certain pattern; but it can be said that the better cancellation is obtained by higher-value currents. Also the circuit works better for 1 MHz as the suppression reaches $\sim -30dB$.

As mentioned in the previous section, Q_3 is not needed for the circuit and only prevents the capacitance of the signal photodiode from loading the summing junction. Fig. 2.8 shows the performance of this circuit without the cascode transistor Q_3 for different powers of the signal beam. By comparing Fig. 2.7 and Fig. 2.8, it can be concluded that the cascode transistor improves the cancellation performance.

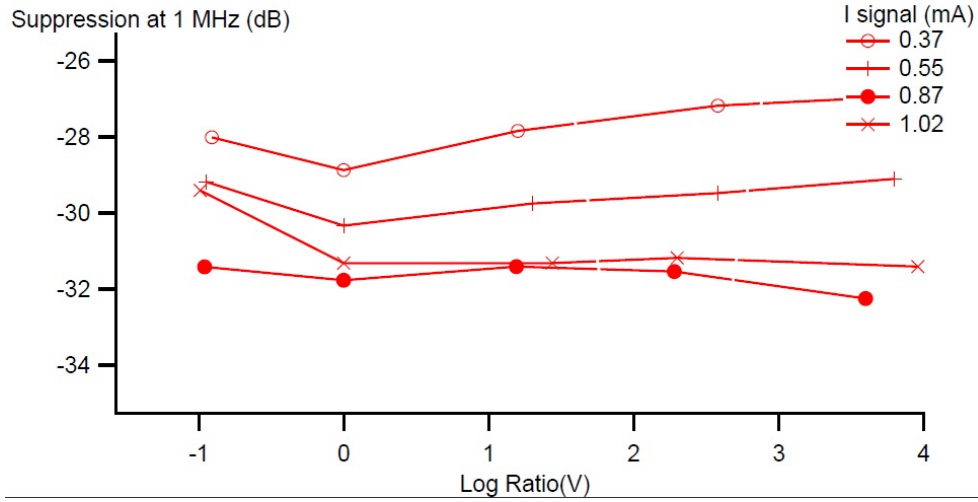


Figure 2.6: Measured 1 MHz cancellation performance of the circuit of Fig. 2.5 with THAT340 transistors as a function of the log ratio output voltage.

To investigate the improvement of the circuit, $0.2 \mu\text{F}$ is used instead of $2\mu\text{F}$ in the feedback part of the circuit and the suppression by the circuit is shown in Fig. 2.9.

Comparing Fig. 2.9 with Fig. 2.7 proves that using $0.2 \mu\text{F}$ improves the suppression by 5 dBm. In Fig. 2.10 the cancellation performance of the circuit of Fig. 2.5 is shown using HFA3096BZ-ND transistors. NPN and PNP transistors have $h_T = 8 \text{ GHz}$ and $h_T = 5.5 \text{ GHz}$ respectively. Consequently, HFA3096BZ-ND is selected for use in the noise cancellation circuit of the experiments since its cancellation capability is the highest among all of the transistors used.

It is important to mention that LTSPICE (analog circuit simulation) could not predict the performance of the noise cancellation circuit. For example, the LTSPICE simulation showed that the cancellation with THAT 340 transistors would be better than with the HFA3096BZ-ND transistors, while the results of the experiments were opposite.

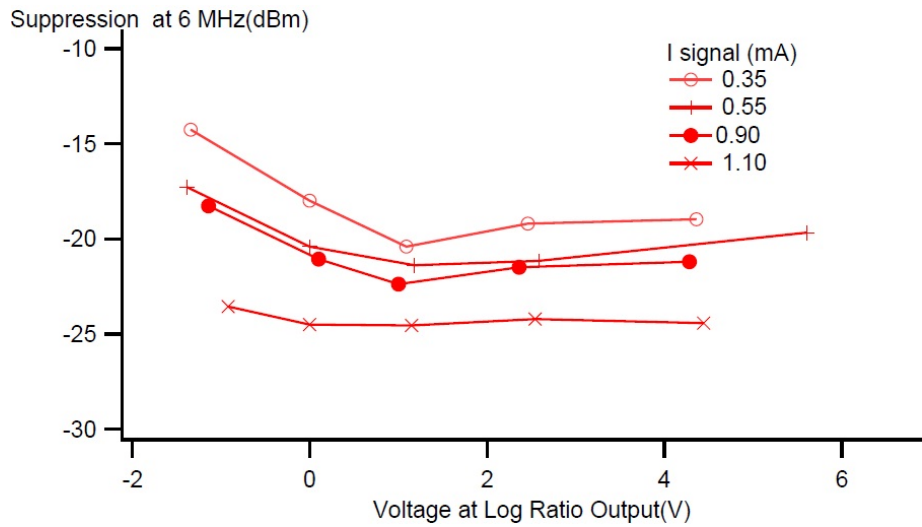


Figure 2.7: Measured 6 MHz cancellation performance of the circuit of Fig. 2.5 with THAT340 transistors as a function of the log ratio output voltage.

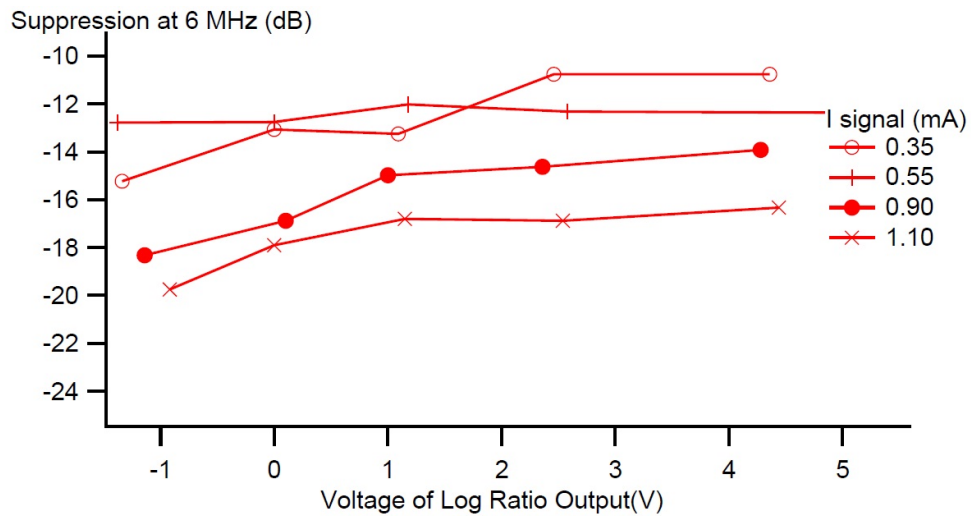


Figure 2.8: Cancellation performance at 6 MHz of the circuit of Fig. 2.5 without cascode transistor Q_3 . THAT340 is used for Q_1 and Q_2 (two NPNs).

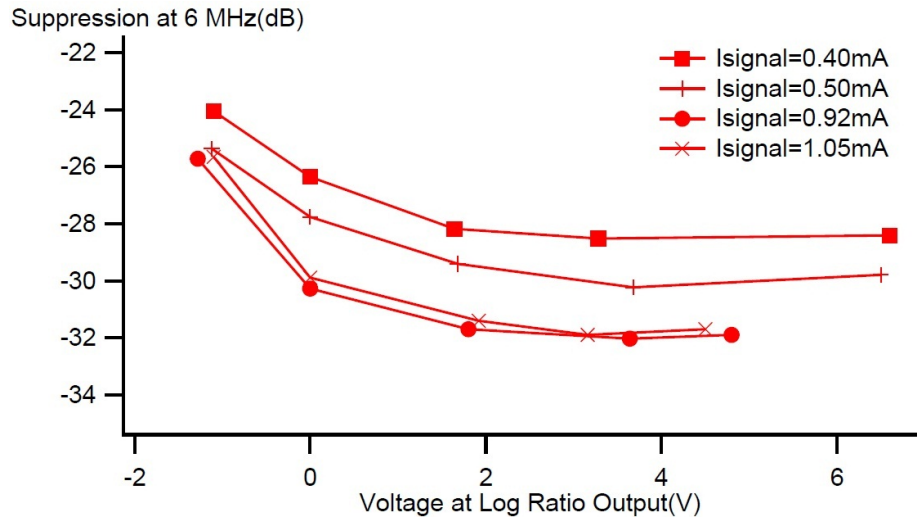


Figure 2.9: The suppression of the signal by the circuit of Fig. 2.5 which used $0.2 \mu\text{F}$ instead of $2 \mu\text{F}$ in the feedback part.

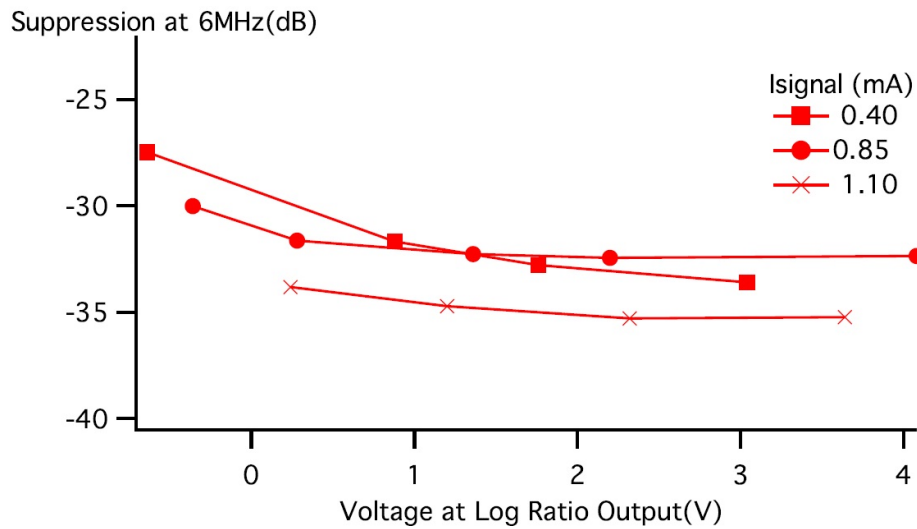


Figure 2.10: The performance of the circuit of Fig. 2.5 with HFA3096BZ-ND transistors.

Chapter 3

Locking System

3.1 Introduction

As more applications need frequency stabilized lasers, this topic has become important and number of innovative methods have been developed [20]. It is convenient to use atomic or molecular transitions directly as the wavelength reference. However these are not often available at the wavelength of interest. Frequency offset locking uses a stabilized reference as a source of stability. As electronic inputs are provided for most modern lasers for tuning purposes, any measured drift frequency can generate an error signal and convert it to a correction signal which can be fed into the laser's electronic tuning inputs and adjust the output frequency. In this technique another laser which is locked to an absolute reference can work as a reference for comparison. Beat note frequency and transfer cavity techniques can be used to stabilize lasers at small and large frequency differences respectively [3], [21]. In frequency stabilization using an optical cavity method, special circuits or computers compare the fringe position of the target laser with its reference [22], [23], [3].

In this chapter, an improvement for diode laser stabilization by the transfer cavity

method will be demonstrated by applying the Pound-Drever-Hall locking system. For this purpose, a new system for generating the laser current modulation will be introduced.

3.2 Optical Cavity Stabilization

A way to monitor laser frequency is to detect what gets transmitted or reflected when a laser beam is sent to a Fabry-Perot cavity. Only light whose frequency is an integer number times the cavity's free spectral range can pass through the cavity. The cavity's free spectral range is defined as $\Delta\nu = c/2L$ where L is the length of the cavity and c is the speed of light [24]. It is possible to have multiple resonance frequencies by fixing the length of the Fabry-Perot cavity. The reference laser's stabilization can be transferred to the target laser by adjusting the length of the cavity appropriately. The cavity is locked to the reference laser, and then the stabilized cavity can be set as a stable reference to lock the target laser [23].

However this technique can only look at the target laser to within one free spectral range of the desired frequency. To avoid this problem the frequency of one laser can be shifted by frequency modulating it to produce sidebands. Therefore the target laser is stabilized such that one of the modulated sidebands matches a resonance of the reference cavity which is stabilized to the reference laser [22]. It is also possible to apply the modulation to the reference laser [3]. This method gives tunability to the transfer cavity stabilization system (see Fig. 3.1).

This method was recently used to lock a 960 nm commercial ring Ti:sapphire laser. A Fabry-Perot transfer cavity is stabilized using a tunable sideband from a current modulated diode laser (slave laser) which was used to stabilize the 960 nm laser [3]. Figure 3.2 shows

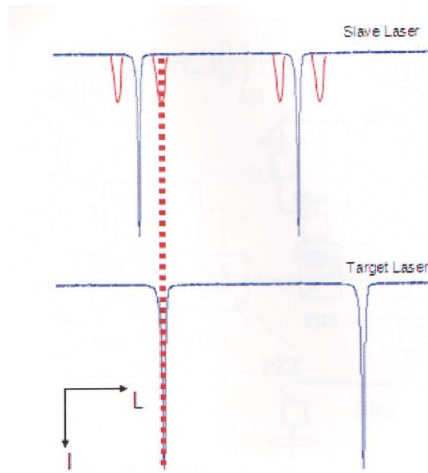


Figure 3.1: Adding a tunable sideband to one laser making the fringes coincide.

the experimental set up which implemented this method. The master (reference) 780 nm laser was locked by polarization spectroscopy.

The error signal is derived from the transmission maximum for both the slave laser's sideband and target laser's frequency. Both laser beams with orthogonal polarizations pass through the cavity and then a polarizing beam splitter separates them at the end of the cavity. The cavity length is dithered at 1.6 kHz by an amplitude of the order of the cavity line-width. The error signal is deduced from the frequency of the dithering by lock-in amplifiers [3]. The 780 nm (slave) error signal is fed back to a control system which adjusts the cavity length using a PZT on one of the end cavity mirrors. The 960 nm (target) error signal is fed back to another control system which tunes the frequency of that laser. By implementing this technique, the frequency of a target laser can be stabilized, with a drift smaller than 1 MHz/hour [3].

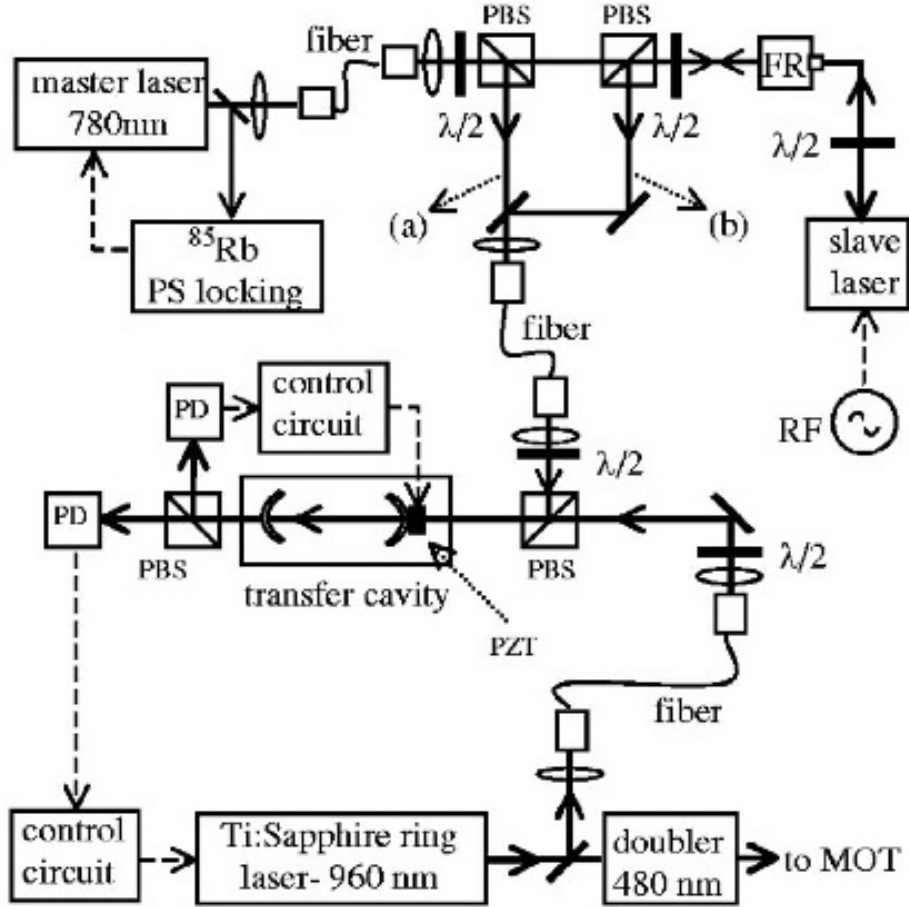


Figure 3.2: Experimental setup employed by Bohlouli-Zanjani et al [3]

3.3 The Pound-Drever-Hall Laser Frequency Stabilization System

Using the transmitted beam to generate an error signal from a Fabry-Perot transfer cavity can be difficult when the intensity of the transmitted light changes. The system can not distinguish the source of any fluctuations which can be fluctuations of the frequency or the intensity of the laser itself [25]. Also by locking the transmitted light to its maximum value, any change in its intensity does not give information about the direction of these

fluctuations. A noise cancellation circuit for measuring the transmitted light can overcome the first problem. The half-maximum intensity on one side of the peak can be set as the zero of the error signal location to make system sensitive to the direction of the frequency fluctuations [26], otherwise the derivative of the transmission peak can be rapidly dithered about the transmission maximum by dithering the cavity length [3].

Measuring the reflected intensity and keeping that at zero is one of the basic concepts that is used in a powerful technique called "Pound-Drever-Hall" locking to improve the laser's frequency stabilization [25]. Since the intensity of the reflected beam has a symmetric shape about the cavity's resonant frequency, the derivative of the intensity can be used instead. To understand how Pound-Drever-Hall works, the response of the reflected beam can be discussed considering a small variation in the frequency. If the frequency value exceeds the resonance frequency, the derivative is positive. It means if the frequency of the laser modulates sinusoidally over a small range, the reflected intensity will also vary sinusoidally. Below the resonance frequency, this derivative is negative. Measuring the derivative of the reflected beam with respect to the frequency can be considered as an error signal and fed back to the laser to lock the laser at resonance [27].

In other words, when the carrier frequency of the laser is matched to the cavity resonance frequency, there is a standing-wave field at that frequency. The measured reflected beam consists of the leakage field and the promptly reflected beam. The promptly reflected beam is also a part of the light which reflects from the first mirror of the cavity and never enters the cavity. Both the leakage field and the promptly reflected beam have the same frequency and almost the same intensity. Since at exact resonance of the cavity the promptly reflected beam and the leakage beam are exactly 180 degrees out of phase, the total reflected beam vanishes. With a slight change in the frequency value, this phase difference between the beams is not exactly 180. Therefore there is some light that reflects from the cavity which shows whether this frequency is higher or lower than the resonant

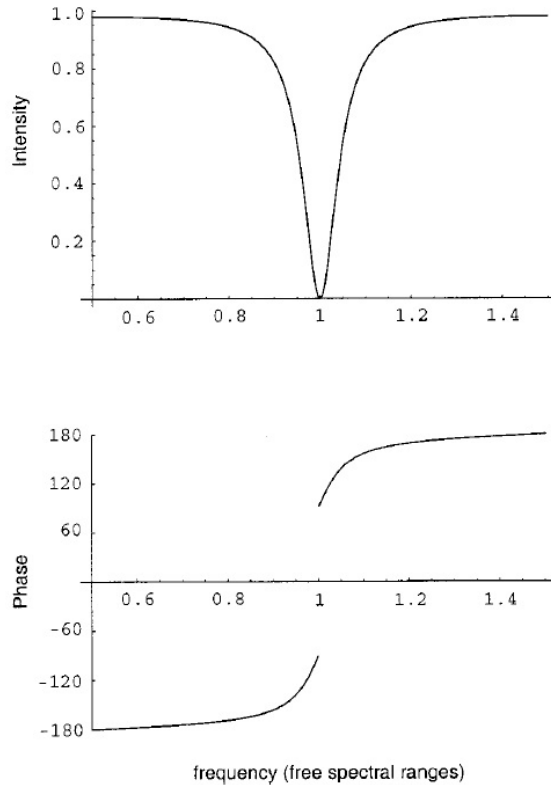


Figure 3.3: Intensity and phase of the reflection beam for Fabry-Perot cavity (from Ref. [27]).

frequency [27], [25]. Fig. 3.3 shows the intensity and phase of the reflected beam near the resonance. The Pound-Drever-Hall technique provides a way to measure the phase of the reflected beam. By frequency-modulating the laser before entering the cavity at Ω , there will be two sidebands with an exact phase relation. This frequency is usually chosen such that the first order sidebands are well outside the transmission line. These sidebands can be totally reflected from the input cavity mirrors. Measuring the reflected beam means the interference of these sidebands with the carrier is measured. This interference makes a beat pattern at the modulation frequency. The phase of this beat note provides the phase of the reflected beam. The phase sensitive demodulation of this beat note pattern induces the desired antisymmetric derivative of the frequency [28]. (For further details please see

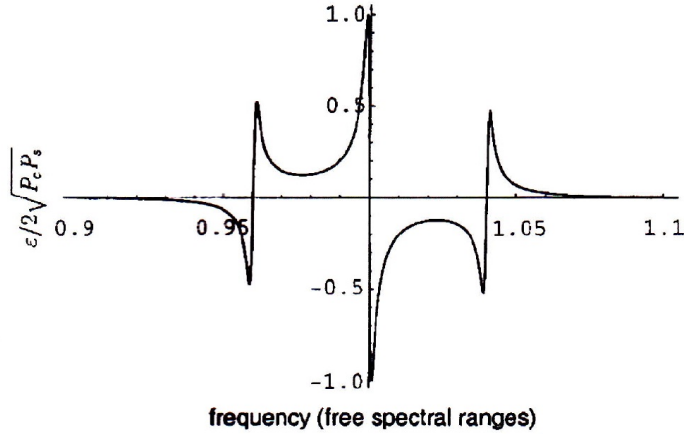


Figure 3.4: The Pound-Drever-Hall error signal for high modulation frequency and ideal phase condition from Ref. [27]

Ref. [25]).

3.4 Using the PDH System to Stabilize an Optical Cavity by a Doubly Current Modulation Injection Locked Diode Laser

Stabilization using the transfer optical cavity mentioned in Section [3.2] is limited in bandwidth since the optical cavity is mechanically dithered. This method can be improved by implementing the Pound-Drever-Hall system. The cavity is locked to one of the sidebands which are made by current-modulating of stabilized laser (slave laser). Furthermore the target laser will be locked to the cavity. By employing the Pound-Drever-Hall system each laser should be modulated instead of dithering the optical transfer cavity. The signal should make a tunable sideband on the carrier which has two fixed frequency ($\sim 10MHz$) sidebands suitable for PDH locking. This current can be written as:

$$I = I_0 \sin(\Omega_1 t + \alpha \sin(\Omega_2 t)). \quad (3.1)$$

As shown below, this current can modulate the phase of the laser:

$$\bar{E} = \frac{E}{E_0} e^{i(\omega t + \beta(\sin(\Omega_1 t + \alpha \sin(\Omega_2 t)))}. \quad (3.2)$$

Where \bar{E} is the normalized complex electric field that can be expanded into its Fourier component. By keeping only the first order of the first modulation it can be written as:

$$\bar{E} = J_0(\beta) e^{i\omega t} + J_1(\beta) [e^{i((\omega + \Omega_1)t + \alpha \sin(\Omega_2 t))} - e^{i((\omega + \Omega_1)t - \alpha \sin(\Omega_2 t))}]. \quad (3.3)$$

This expression shows only the carrier, the first term and the next two terms for one of the first modulation sidebands ($\omega + \Omega_1$). As explained before, the cavity will be locked on the modulation sideband ($\omega + \Omega_1$). The second term of (3.3) can be expanded to first order and becomes:

$$E_{\omega + \Omega}^- \approx J_1(\beta) J_0(\alpha) e^{i(\omega + \Omega_1)t} + J_1(\beta) J_1(\alpha) [e^{i(\omega + \Omega_1 + \Omega_2)t} - e^{i(\omega + \Omega_1 - \Omega_2)t}]. \quad (3.4)$$

With this FM modulation signal, these secondary sidebands can be used in the Pound-Drever-Hall system with the primary sideband at $\omega + \Omega_1$ acting as the carrier. Figure.3.5 shows a schematic of this system.

In practice when a diode laser is frequency-modulated by a current, there will be a residual amplitude modulation that is superimposed on the frequency modulation. The amplitude modulation produces in-phase sidebands in contrast to the frequency modulation which produces out-of-phase sidebands. This contrast results in an amplitude asymmetry of the two sidebands (upper and lower) [30], [31].

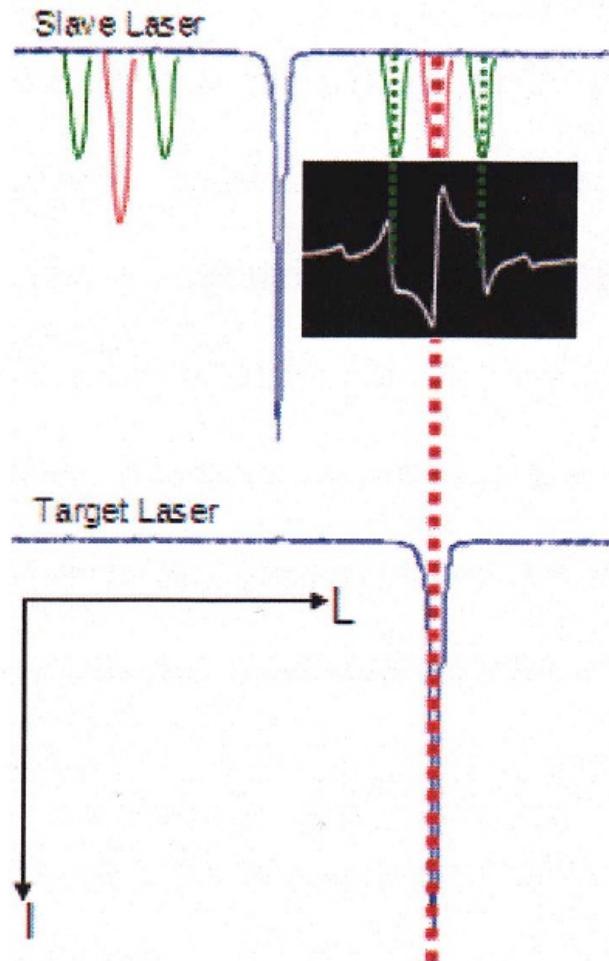


Figure 3.5: Schematic of how the Pound-Drever-Hall method is applied to stabilize the transfer cavity using the secondary sidebands (green) as a PDH sidebands for a primary tunable sideband (red) of the slave laser (from Ref. [29]).

3.5 Modulation Signal Generation

Since the error signal in the Pound-Drever-Hall system only needs the first order frequency modulation sidebands, (3.1) can be written as:

$$I = I_0(\sin(\Omega_1 t) + C_1 \sin(\Omega_1 + \Omega_2) + C_2 \sin(\Omega_1 - \Omega_2)). \quad (3.5)$$

where C_1 and C_2 are constants. To generate this signal, an arbitrary waveform function generator can be used. Most generators are not applicable in this case since they are limited to an upper frequency and the required tuning range is higher than this limit (half free spectral range of the cavity $\sin 400MHz$). The idea to overcome this limitation is synthesizing the arbitrary wave form to a determinate frequency (up-conversion) and then transferring that to a desired variable frequency(down-conversion). It is important to notice that the down-converting process should be tunable to gives the final modulation signal a desired tuning range, however the frequency of up-converting is fixed.

3.5.1 Generating Waveform

An arbitrary waveform generator (Agilent, 33220A) generates the signal as following(note that Ω_1 and Ω_2 are defined differently from the previous section):

$$V = V_0(\sin(\Omega_1 t) + C_1 \sin(\Omega_1 + \Omega_2) + C_2 \sin(\Omega_1 - \Omega_2)). \quad (3.6)$$

C_1 and C_2 are chosen such to maximize the overall amplitude of the error signal. In this experiment C_1 and C_2 are equal to 0.40 and 0.38 respectively. Also the frequencies of the carrier Ω_1 and sidebands $\Omega_1 \pm \Omega_2$ must be integer multiples of one certain frequency since the arbitrary waveform generator operates by looping the arbitrary waveform at that frequency [29]. The base frequency is chosen as 2.25 MHz in order to prevent interference from known RFI sources. Since the three output frequencies are 4, 6 and 8 times of the base frequency, Ω_1 is 9 MHz and Ω_2 is 4.5 MHz.

3.5.2 Transferring

The easiest way to shift a signal to a desired frequency is to mix that with a pure sine waveform. By implementing this main idea, the two-step process can transfer the arbitrary waveform to the desired frequency. In the first step the waveform is up-converted to a certain very high frequency which is higher than the desired frequency. This is then down-converted to the desired frequency [29].

In the first step (single sideband up-conversion) the waveform is split into two parts such that one of them has a 90° phase shift. Both parts are separately mixed with the same pure sine waveform that has a fixed frequency. At the end, both parts are added together as one of them has a 90° phase delay. This produces a single sideband. As shown in Fig. 3.6 the arbitrary waveform is split by the first phase splitter (Mini-Circuits, ZSCQ-2-90), and each part goes through a mixer (Mini-Circuits, ZP-5X) to be mixed with the sine wave made by the voltage-controlled oscillator VCO (Mini-Circuits, ZX95-748+) at 813 MHz. Then they are united through the second phase splitter (Mini-Circuits, ZSCQ-2-90).

After single sideband up-conversion the signal is down-converted to the desired tuning range through mixing (Mini-Circuits, ZP-5X) with a tunable frequency output from a signal generator (Agilent, E8267D).

It is important to mention that since the demodulation frequency is Ω_2 , a convenient source of this frequency that has a locked phase relationship with the modulation signal is needed. For this purpose we use the Sync output of the arbitrary waveform generator (Agilent, 33220A) can help to have the locked phase relationship. Since the Sync output is a square wave at the base frequency of 2.25 MHz, a low pass filter (Mini-Circuits, PLP-2.5+) is used before a frequency multiplier (Mini-circuits, MK-3) and another low pass filter (5 MHz) to produce a pure sine wave at 4.5 MHz for demodulation. Part b of Fig. 3.6 shows this configuration.

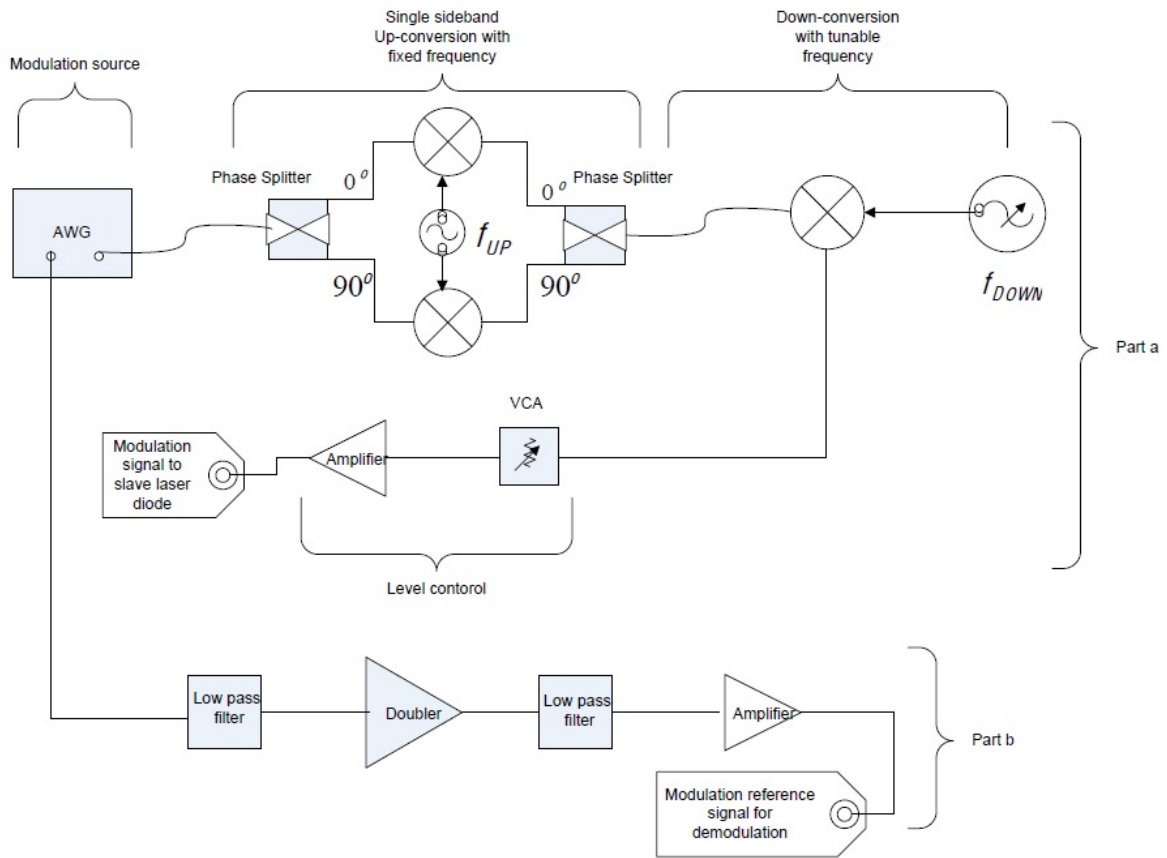


Figure 3.6: Part a: The system for generation of the slave laser current modulation. AWG: Arbitrary waveform generator, VCA: Voltage controlled attenuator. Part b: The system for preparing the reference signal for demodulation.

3.6 Current Modulation of the diode laser

The modulation signal which was explained in the previous section is applied for current modulation of the injection locked slave laser. It is known that with a high power of modulation, the injection locking of the slave laser fails. However the modulation strength directly influences the strength of the error signal. By directly current modulating the diode laser using a synthesizer, it was found that a power of more than 14 dBm for the frequency range of 100-600 MHz can cause the injection lock to fail. The modulation signal power is adjusted by means of an amplifier (Mini-circuits, ZKL-2R7) and a voltage variable attenuator (Mini-Circuits, ZX73-2500+) as shown in Fig. 3.6. It is important that the gain of this amplifier does not change significantly for the desired frequency range. Given an 8 V input for the variable attenuator the carrier signal's power can be 12 dBm for injection into the diode laser.

Chapter 4

Experiment

As mentioned in the previous section, the Pound-Drever-Hall system is applied to improve the optical transfer cavity stabilization using current modulated injection-locked diode lasers. In this chapter the experimental set up to implement this system as well as the noise cancellation circuit and some measurements will be discussed.

4.1 Experimental Setup

This method was developed for a 775 nm external cavity diode laser. This laser can also be locked by transmission through the Rb cell. This will be used to check the PDH cavity locking system. The frequency-stabilized 780 nm laser is the reference for the transfer cavity stabilization. The locking scheme is as follows: The master (reference) 780 nm laser is locked by saturated absorption spectroscopy. A small part of this laser is employed for injection locking of the 780 nm slave laser. Injection locking is checked using a Fabry-Perot cavity. The RF current modulation is applied to the slave laser as explained in section [3.5]. The carrier frequency of the modulation is chosen such that a transmission peak of the slave laser coincides with a 775 nm transmission peak. Furthermore by stopping the

cavity ramping, the cavity will be locked to the sideband of the 780 nm reflected beam. Moreover, the 775 nm laser will be locked to its own reflected beam. The PDH method is used for locking both systems. The locking point can be changed by scanning the carrier frequency of the slave laser modulation. The experiment is repeated two times: at first the noise cancellation circuit is used only for the 780 nm locking system. In the second case it is used for both systems.

Figure 4.1 shows the experimental setup. The reference laser is a grating stabilized diode laser (Toptica, DLX110) with an external cavity operating at 780 nm. A fine tuning of this laser is achieved using a PZT. Its beam becomes linearly polarized by an isolator just after the laser. A small part of this beam is used for the frequency locking by Rb saturation absorption spectroscopy [32]. The injection locking of the slave laser is performed by means of the remaining part of this laser beam.

The slave laser is a commercial 780 nm diode laser (Sanyo, DL7140-201S) in a temperature stabilized mount (Thorlabs, TCLDM9). Some part of the slave laser goes to a cavity to verify the injection lock. The rest of it is coupled into a single mode fiber. Before going to the fiber, it is passed through a half wave plate and a polarizing beam splitter (PBS) to have a well defined polarization.

The external cavity target diode laser is in a temperature stabilized mount at 13.5°C which operates at 775 nm. This laser can be tuned manually by changing the grating angle, while for precise adjustment a PZT is used. In high humidity, nitrogen gas must flow into the laser box to prevent water condensation inside the cavity. This laser is frequency modulated at 5.3 MHz with -23 dBm using a waveform generator (HP, 33120A). For absorption spectroscopy, 6 mW of this laser is directly passed through a Rb cell. As explained in Section [1.2], 7mW of the 780 nm reference laser is simultaneously passed through the Rb cell in the opposite direction for the two-photon spectroscopy. The Rb

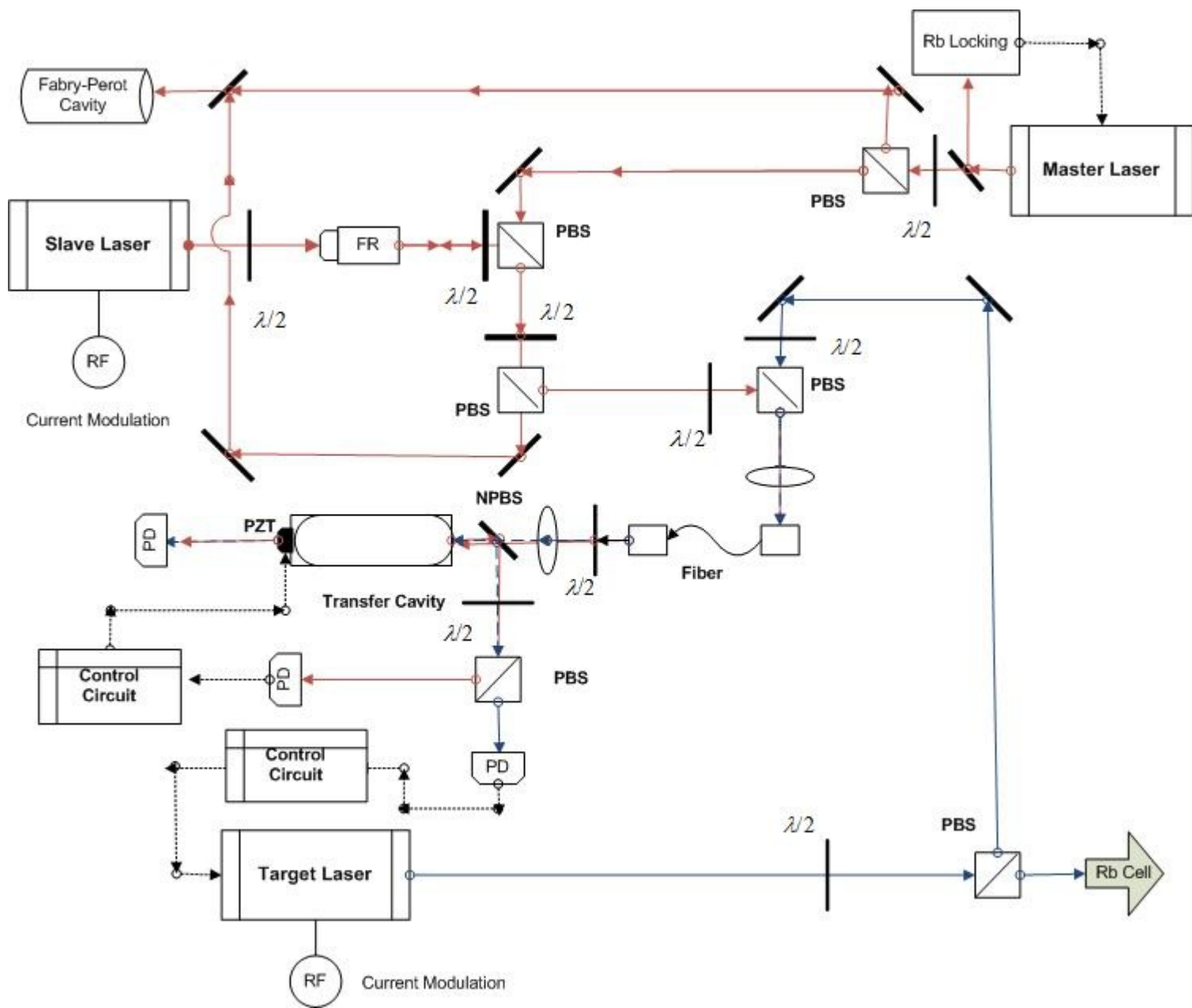


Figure 4.1: Experimental setup. PBS: polarizing beam splitter, PD: photodiode, FR: Faraday rotator, NPBS: None-polarizing beam splitter.

atoms are excited at first by 780 nm from $5s \rightarrow 5p$ and then by 775 nm $5p \rightarrow 5d$. This is used to check the stability of the cavity locking system.

The remaining part of the target laser is coupled to the fiber. The purpose of using the fiber is to make the two laser beams parallel with the same size. At first, the position of the fiber is adjusted for the 775 nm laser beam by changing the X-Y and Z positions of the fiber. It should be noted that adjusting the angle of the beam by mirrors can help to maximize the efficiency. The second laser beam, 780 nm must be aligned with respect to the adjusted position of the fiber. The maximum efficiency for 775 nm is 50 percent and for 780 nm laser beam is 48 percent. Just before the cavity, those beams are divided into two parts by using the 50:50 non-polarizing beam splitter (ThorLabs, BSW05). One of these parts is employed as a reference for the error signal as explained in Section [2.2].

The transfer cavity is the confocal Fabry-Perot type, consisting of two mirrors with a radii of curvature of $R = 0.092m$ and free spectral range of 815 MHz. High reflectivity at the two wavelengths is required to have a high finesse. A standard coated dielectric mirror (Newport, BD2) is chosen to have high reflectivity (≈ 0.997). A PZT is attached to one of the end mirrors. The basic requirement to mode-match the Fabry-Perot cavity is to adjust the beam exactly along the optical axis (the line connecting the center of two mirrors). Also a lens must be used to focus the beam into the center of the cavity. The optimum size of the beam at the center of the cavity is determined by maximizing the degree of the mode-matching to the angular and transitional error in the alignment of the laser beam and the cavity [33]. Based on this calculation, the spot size must be $\omega_0 = \sqrt{\frac{L\lambda}{2\pi}}$ where L is the length of the cavity. This spot size is $107 \mu m$ for the 780 nm laser. By some geometric optics calculations, it is found that the focal distance of the mode-matching lens must be 6.5 cm which is placed 27 cm far from the cavity (the first end mirror). The transmitted light from the cavity which is detected by a photodiode is used to verify the single mode

operation.

After the orthogonally polarized 775 nm and 780 nm laser beams reflect from the cavity, they are separated by a polarizing beam splitter. Then as mentioned, the 780 nm beam is sent to the noise cancellation circuit and the 775 nm beam is directed onto a photodiode (ThorLabs, SM05PD2A) biased through a bias-T (Mini-Circuit, ZFBT-6GW).

It is important to mention that the beams are separately demodulated by mixing them with their own modulation signal which is the same modulation signal for the 775 nm beam and is a pure sine wave at 4.5 MHz for the 780 nm beam as explained in Section[3.5]. Consequently a derivative-like line-shape error signal is provided for locking each reflected beam. An integrator control loop is used for the 780 nm error signal to adjust the cavity length. The 775 nm laser is locked to the cavity.

Initially during the experiment, it is found that a small part of reflected light from the cavity goes back into the fiber and makes undesired feedback. To avoid this problem, an isolator can be used just after the fiber. But in the experiment, two orthogonal beams are required, so it is not possible to use an isolator. The fiber did not have low optical return loss for both two ends. Using a fiber with high return loss for both ends can help to avoid undesired feedback. A new fiber with properties similar to the former one, was used in the experiments. This fiber (ThorLabs, P3-780PM-FC-5 - Patch Cable) has 60 dB optical return loss for both end ports. An 11-mm lens must be used for the output end of this fiber to have the same beam size and mode-matching with the cavity.

Figure 4.2 shows the error signal for the reflected beam of the 780 nm (slave) laser for four different modulation frequencies.

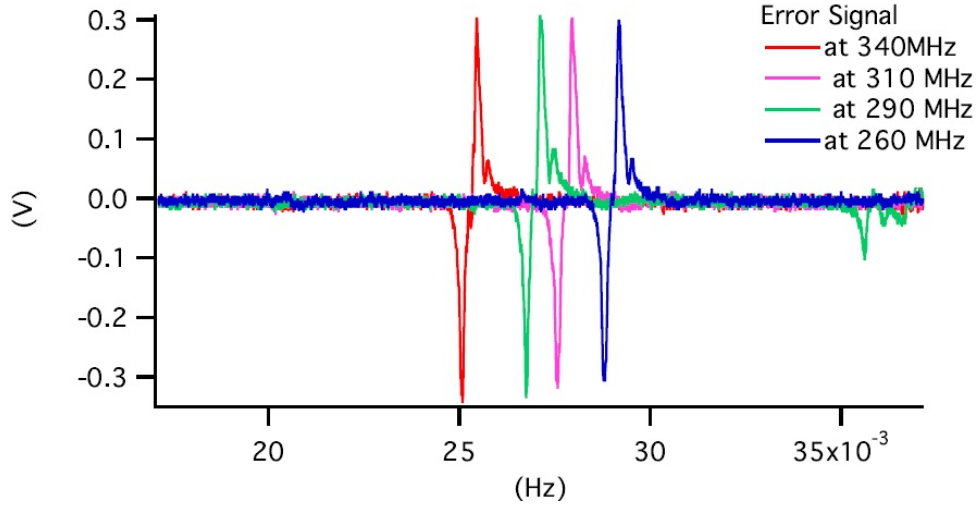


Figure 4.2: The error signal of reflected beam for the 780 nm laser with different frequencies of modulation using the noise cancellation circuit.

4.2 Measurements

When the 775 nm laser is locked, its frequency may be changed by scanning the carrier modulation frequency Ω_1 . The absorption spectrum for the $5p_{3/2}$ to $5d_{5/2}$ transition of ^{87}Rb and its error signal are shown in Fig. 4.3.

By scanning the frequency over the absorption spectrum and recording the main peak position, the frequency drift of the locked 775 nm laser can be monitored. While the locking system is working, the modulation frequency of the 780 nm laser was adjusted up and down by 3 MHz a couple of times to produce calibration fiducials. Figure (4.4) shows the stabilized behavior of the locking system.

In addition to the target laser drift, slave laser drift can limit the long term stability. As mentioned before, the experiment was repeated using the noise cancellation circuit for both lasers (Fig. 4.5 and 4.6).

The purpose of these measurements is to show that using the noise cancellation circuit can improve the locking system. Although they show the locking system works, there is

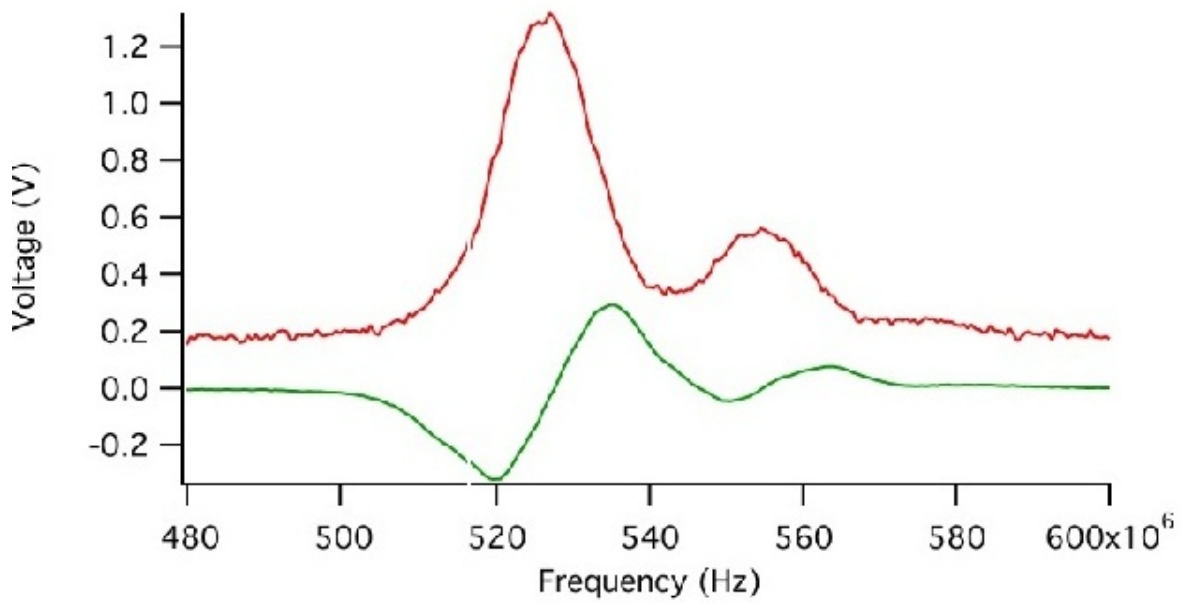


Figure 4.3: Absorption spectrum for the $5p_{3/2}$ to $5d_{5/2}$ of ^{87}Rb transition and the associated error signal obtained by scanning the carrier modulation frequency of the slave laser. In this measurement the noise cancellation circuit is used only for the 780 nm laser

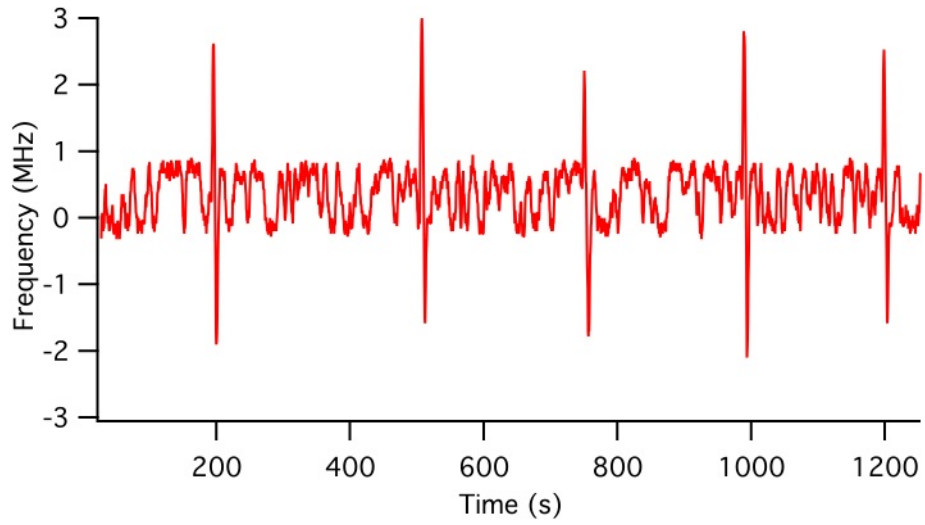


Figure 4.4: Drift frequency of the 775 nm laser over time. In this measurement the noise cancellation circuit was used only for the 780 nm laser

insufficient data to assess the effectiveness of noise cancellation in this application.

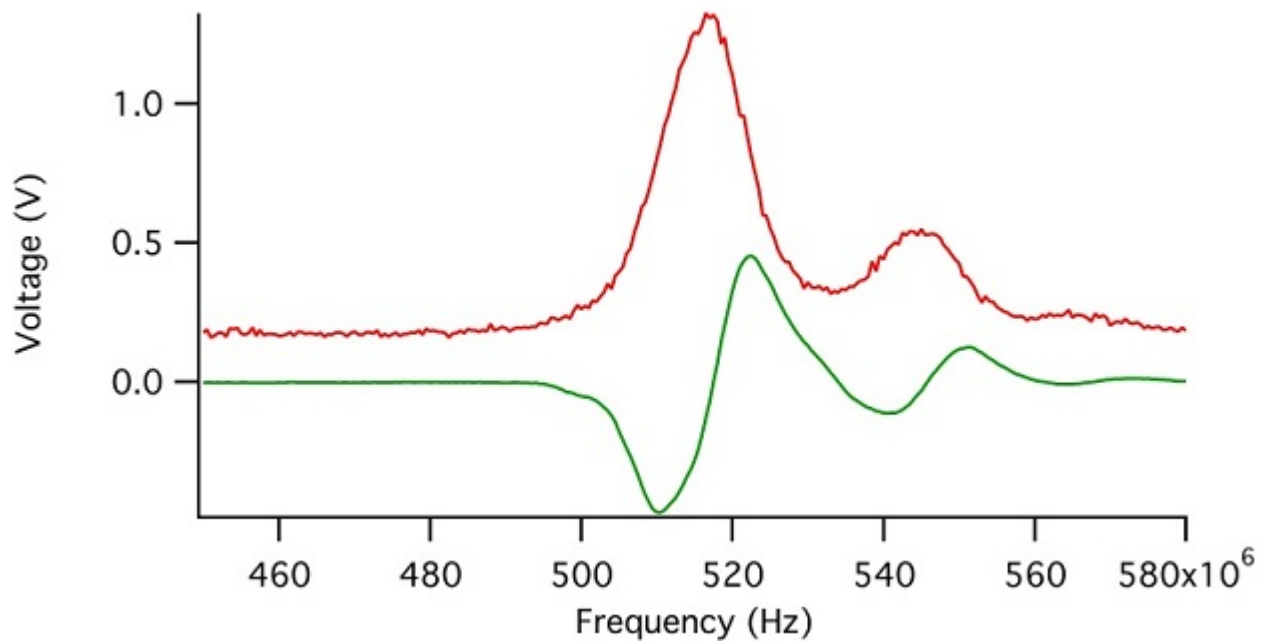


Figure 4.5: Absorption spectrum for the $5p_{3/2}$ to $5d_{5/2}$ transition of ^{87}Rb and the associated error signal obtained by scanning the carrier modulation frequency of the slave laser. In this measurement the noise cancellation circuits are used for measuring both the 780 nm and 775 nm lasers

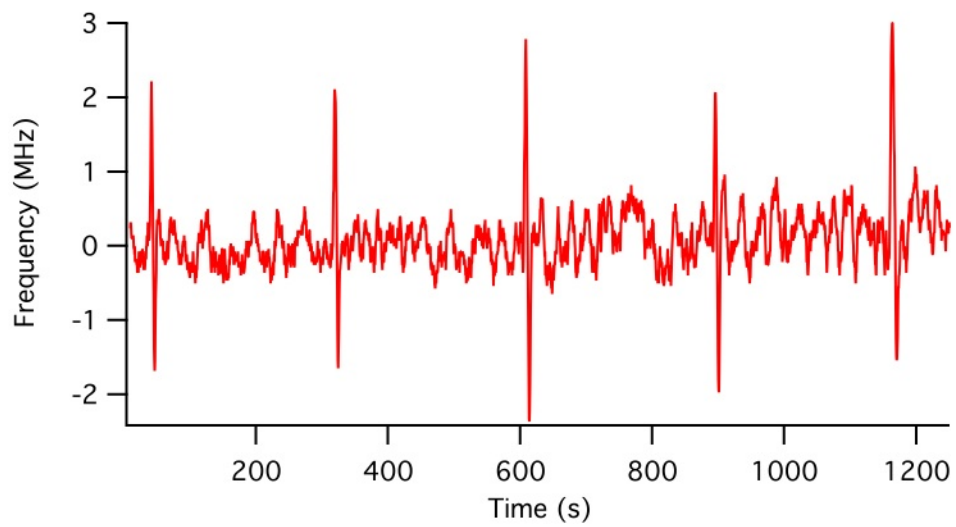


Figure 4.6: Drift frequency of the 775 nm laser over time. In this measurement noise cancellation circuits are used for both the 780 nm and 775 nm lasers

Chapter 5

Summary and Suggestions for Future Works

A three-step Rydberg excitation method using diode lasers was explained. The transitions from $5s_{1/2}$ to $5p_{3/2}$ and from $5p_{3/2}$ to $5d_{5/2}$ in ^{87}Rb were accomplished by frequency stabilized diode lasers at 780 nm and 775 nm. For the last step of the excitation, a 1260 nm frequency-stabilized diode laser is required. To improve the stabilization method, the Pound-Drever-Hall system was used for transfer cavity stabilization. Both target and reference lasers were frequency-modulated by current modulation. Employing the second sideband of the modulation for the reference laser the transfer cavity was locked. The target laser was stabilized by locking that to the stabilized cavity.

To check this method, a 775 nm external cavity diode laser is used instead of a 1260 nm diode laser. Both the target and slave lasers were current-modulated. A special method was introduced to generate the required slave laser modulation signal. Residual intensity modulation creates an undesired baseline in measurements. Previously the signal was subtracted from the reference beam to suppress this baseline. This method was improved using

a negative feedback signal as implemented by a noise cancellation circuit. The noise cancellation circuit provides continuous adjustment of the DC balance between the signal and comparison beams. As a result, -35 dB suppression of the residual intensity modulation was reached.

By applying these improvements to the locking method, the 1260 nm diode laser will be locked to the stabilized transfer cavity. The 1260 nm laser will excite the rubidium atoms to the f series of the Rydberg states. Consequently interactions of these excited atoms with metal surfaces will be investigated.

It is recommended to use a proper filter for each beam laser before photodiodes. This will help to prevent any interference in measurements. Based on the experience gained during these experiments, fibers with high optical return losses should be used.

In measurements with the noise cancellation circuit, it is suggested to apply a comparison beam with a power more than twice the signal beam. This condition will result in better suppression.

Bibliography

- [1] T. F. Gallagher, *Rydberg Atoms*. Cambridge University Press, 1994.
- [2] D. Kleppner, M. Littman, and M. Zimmerman, *Rydberg states of atoms and molecules*. 1983.
- [3] P. Bohlouli-Zanjani, K. Afrousheh, and J. D. D. Martin *Review of Scientific Instruments*, vol. 77, pp. 093105–1, September 2006.
- [4] P. Bohlouli-Zanjani, J. A. Petrus, and J. D. D. Martin *Physical Review Letter*, vol. 98, 2007.
- [5] R. Mantifel, “Rydberg state excitation using diode laser,” *Physics 437B Report*, University of Waterloo, Waterloo, ON 2007.
- [6] F. Nez, F. Biraben, R. Felder, and Y. Millerieux *Optics Commun.*, vol. 102, pp. 432–438, October 1993.
- [7] C. E. Wieman and L. Hollberg *Review of Scientific Instruments*, vol. 62, pp. 1–20, January 1990.
- [8] M. W. Fleming and A. Mooradian *Appl. Phys. Lett*, vol. 38, no. 7, pp. 9191–9197, 1981.

- [9] K. B. MacAdam, A. Steinbach, and C. Wieman *American Journal of Physics*, vol. 60, pp. 1098–1111, December 1992.
- [10] A. J. Olson, E. J. Carlson, and S. K. Mayer *American Journal of Physics*, vol. 74, pp. 218–223, March 2006.
- [11] T. T. Grove, V. Sanchez-Villicana, B. C. Duncan, S. Maleki, and P. L. Gould, “Two-photon two-color diode laser spectroscopy of the rb $5d_{5/2}$ state,” *Physica Scripta.*, vol. 52, pp. 271–276, 1995.
- [12] W. Suptitz, B. C. Duncan, and P. L. Gould *Journal of the Optical Society of America B*, vol. 14, pp. 1001–1008, May 1997.
- [13] R. W. P. Drever and et al., “Laser phase and frequency stabilization using an optical resonator,” *Applied Physics B*, vol. 31, pp. 97–105, 1983.
- [14] P. C. D. Hobbs *Applied Optics*, vol. 34, pp. 1579–1590, March 1994.
- [15] P. C. D. Hobbs *Applied Optics*, vol. 36, no. 4, pp. 903–920, 1997.
- [16] R. L. Forward *Appl. Phys. Lett.*, vol. 17, no. 2, p. 379390, 1977.
- [17] P. C. D. Hobbs *Optics and Photonics News*, pp. 17–22, April 1991.
- [18] P. C. D. Hobbs *Society of Photo-Optical Instrumentation Engineers*, vol. 1376, pp. 216–221, 1990.
- [19] P. Hobbs, *Building Electro-Optical Systems: Making It All Work*. Wiley Series in Pure and Applied Optics, Wiley, 2009.
- [20] J. L. Hall *Science*, vol. 202, pp. 147–156, October 1978.
- [21] U. Schunemann, R. G. H. Engler, and a. M. Z. M. Weidemuller *Review of Scientific Instruments*, vol. 70, 1998.

- [22] J. Helmcke, S. A. Lee, and J. L. Hall *Applied Optics*, vol. 21, pp. 11686–1694, May 1982.
- [23] W. Z. Zhao, J. E. Simsarian, L. A. Orzco, and G. D. Sprouse *Review of Scientific Instruments*, vol. 69, pp. 3737–3740, November 1998.
- [24] G. R. Fowles, *Introduction to Modern Optics*. Holt, Rinehart and Winston (New York), 1975.
- [25] R. W. P. Drever, J. L. Hall, F. V. Kowalski, J. Hough, G. M. Ford, A. J. Munley, and H. Ward, “Laser phase and frequency stabilization using an optical resonator,” *Applied Physics B: Lasers and Optics*, vol. 31, pp. 97–105, 1983. 10.1007/BF00702605.
- [26] R. L. Barger and et al. *Applied Physics Letter*, vol. 22, pp. 573–575, June 1973.
- [27] E. D. Black *American Journal of Physics*, vol. 69, pp. 79–87, January 2001.
- [28] G. C. Bjorklund *Optics Letters*, vol. 5, pp. 15–17, January 1979.
- [29] I. B. Burgess, “Transfer cavity stabilization using the pound-drever-hall system,” *Physics 437B report*, University of Waterloo, Waterloo, ON 2008.
- [30] S. Koboyashi and T. Kimura *IEEE Journal of Quantum electronics*, vol. QE 18, pp. 421 – 427, April 1982.
- [31] L. Goldberg, F. Taylor, and J. F. Weller *Electronics Letters*, vol. 18, pp. 1019–1020, November 1982.
- [32] D. W. Preston *American Journal of Physics*, vol. 64, no. 11, p. 1432, 1996.
- [33] C. Munnerln and J. W. Balliett *Applied Optics*, vol. 9, pp. 2535–2538, November 1970.